A subsurface pathway for salinity anomalies propagating from the northwestern subtropical Pacific to the eastern Luzon Strait

Youfang Yan[1], Eric P. Chassignet[2], Lingling Liu[3], Yiquan Qi[1]

1 State Key Laboratory of Tropical Oceanography (South China Sea Institute of Oceanology, Chinese Academy of Sciences), Guangzhou, China

2 Center for Ocean-Atmospheric Prediction Studies, Florida State University, Tallahassee, Florida

3 Key Laboratory of Ocean Circulation and Waves, Institute of Oceanology, Chinese Academy of Sciences, Qingdao, China

Abstract

The subsurface ocean signal propagation from subtropics to tropics has been reported to play a vital role in low-frequency climate variability. In this study, monthly gridded temperature and salinity datasets based mainly on Argo profiles for 2003-2012 are used to investigate the subduction and propagation of salinity anomalies along 24.5-25.2 σ_θ isopycnals in the northwestern Pacific. Results from statistic to case studies suggest that prominent salinity anomalies generated in the northwestern subtropical outcropping area (30-35°N, 130-160°E), with their maximum magnitude of about 0.15 PSU, can be subducted in late winter and advected to the eastern Luzon Strait (15°N, 130°E) by southwestward subtropical circulation in roughly one year. In contrast to anomalies generated in the northeastern subtropical Pacific that propagate slowly and dissipate strongly, these anomalies have a noticeable signature along their propagation pathway and quickly impact the subsurface thermohaline structure in the western boundary.

1. Introduction

According to the ventilated thermocline theory (Luyten et al., 1983; Woods, 1985), temperature or salinity anomalies subducted into the mid-latitudes of the North Pacific can be transported to the low-latitude regions via the westward and equatorward gyre circulations. Using historical temperature observations, Deser et al. (1996) showed that temperature anomalies in the eastern subtropical Pacific can be subducted and advected equatorward to the tropics along isopycnals. By performing a trajectory analysis of water parcels in a realistic oceanic general circulation model, Gu and Philander (1997) proposed three main pathways for the transport of subtropical waters to the low latitudes. First, waters subducted into the eastern subtropical Pacific flow equatorward along isopycnal surfaces and subsequently reach the tropics through the interior zigzag window (route I). Second, waters subducted into the central/eastern subtropical Pacific move westward and reach the western boundary, where they bifurcate: part of the waters flow in the form of an equatorward western boundary current (WBC) to the tropics (route II), and part head northward to the mid-latitudes via the poleward WBC (route III). These subducted waters take about 10 years to reach the equator and western boundary, and play a vital role in low-frequency climate variability (Fine et al., 1987; Gu and Philander, 1997).

Because of the general paucity of salinity observations, the above studies mainly focused on the transport of thermal anomalies in the North Pacific. Recently, taking advantage of rapid advances in ocean observations, the high-quality salinity data from Argo floats have provided an invaluable tool to resolve the interannual subsurface salinity variability and their propagation pathways in the North Pacific (e.g., Johnson, 2006; Sasaki et al., 2010; Ren and Riser, 2010; Li et al., 2012a; Yan et al., 2012). Among others, Sasaki et al. (2010) reported that anomalous spiciness (i.e., potential temperature and salinity variation on an isopycnal) generated in the northeastern subtropical Pacific can propagate southwestward and equatorward along 25-25.5 σ_θ isopycnals. However, because of the strong dissipation of the anomaly along its route, it was not able to reach the western boundary and equatorial regions. Li et al. (2012) and Kolodziejczyk and Gaillard (2012) observed remarkable strong attenuation of highly compensated winter water subducted into the northeastern subtropical Pacific.

Instead of tracking anomalies generated in the northeastern subtropical Pacific to determine possible source of communication between the tropics and subtropics, Yan et al. (2012; 2013) investigated the subsurface salinity variability downstream in the eastern Luzon Strait. They found that the observed subsurface salinity anomalies in the eastern Luzon Strait cannot be traced back to anomalies in the eastern basin and that, instead, they were clearly related to salinity anomalies subducted into the northwestern subtropical Pacific (30-35°N, 130-160°E).

Although the connection between the subsurface salinity anomaly in the eastern Luzon Strait and that in the northwestern subtropical Pacific has been proposed by Yan et al. (2012; 2013), the detailed characterization of this anomaly and its propagation pathway are still not clear. How fast does this anomaly propagate? Does it extend to the low-latitude regions? These questions are addressed in the present study to gain more insight into the pycnocline remote connection between the tropics and the subtropics. The remainder of the paper is organized as follows: A brief description of data and method of analysis is presented in section 2; the subduction and propagation pathways of salinity anomalies in the northwestern Pacific are explained in section 3; and results are summarized and discussed in section 4.

2. Data and method

The monthly mean temperature and salinity field compiled by Hosoda et al. (2008), based on high-quality Argo profiles, Triangle Trans-Ocean Buoy Network buoy measurements, and other available conductivity-temperature-depth (CTD) data, is used in this study. This dataset is known as the Grid Point Values of the Monthly Objective Analysis using the Argo data (MOAA GPV). The MOAA-GPV has a 1°×1° spatial resolution for the 2000 m upper ocean and has been widely used to investigate interannual-to-decadal variability in the subtropical Pacific (e.g., Sasaki et al., 2010; Tomita et al. 2010; Li et al. 2012; Qiu and Chen, 2012; Yan et al., 2013). Since data from the subtropical Pacific are reasonably sampled until 2003, the focus of our analyses is on the period 2003-2012. The salinity anomaly in each month is defined as the deviation of the salinity mean over the period of 2003-2012 for each pressure layer.

The Montgomery geostrophic streamfunction referred to 2000 dbar on isopycnal surfaces is calculated following Montgomery (1937) and IOC et al. (2010). The mean surface geostrophic velocities are derived from the MDT_CNES-CLS09 product (Rio et al., 2011). The statistical description of the interannual salinity patterns on any given isopycnal surface is performed with the Extended Empirical Orthogonal Function (EEOF). Compared to the classical EOF analysis, the EEOF analysis can catch the propagating pattern by introducing time lag into the covariance matrix. The annual subduction rate R_{ann}, which is calculated by tracing water parcels released at the base of the winter mixed layer for one year in a Lagrangian framework, is expressed as (Huang and Qiu, 1998):

$$R_{ann} = -\frac{1}{T}\int_{t_1}^{t_2} w_{mb}dt - \frac{1}{T}[h_{\mathrm{m}}(t_2) - h_{\mathrm{m}}(t_1)], \quad (1)$$

where T represents the time period of integration (one year); t_1 and t_2 are the end of the first and second winter, respectively; h_m is the winter mixed layer depth (MLD); and w_{mb} is the vertical velocity at the base of the mixed layer.

3. Isopycnal salinity anomalies and their propagation in the northwestern subtropical Pacific

3.1 Salinity anomalies

The isopycnal salinity anomalies in the northwestern subtropical Pacific have been the subject of many recent studies owing to the Argo float observations (Li et al., 2012a; Yan et al., 2012; 2013; Sugimoto et al., 2013). Because the maximum subduction occurs in the winter, we first show in Fig. 1b the standard deviation (STD) of winter salinity anomalies averaged on 24.5-25.2 σ_θ isopycnals to facilitate comparison with similar previous studies (Yan et al., 2012; 2013). There is a band of large salinity variability in the Kuroshio Extension around 30-35°N, which has a magnitude of up to 0.1 PSU. This salinity anomaly compares favorably with Yan et al.'s (2013) Fig. 7 and spreads along the 24.5-25.2 σ_θ outcrop lines (Fig.1c: cyan curves). The high-variability salinity signature in the outcrop regions of the Kuroshio Extension forms a strong contrast with low-variability salinity anomalies in the tropics and in the eastern Luzon Strait.

Changes of surface freshwater flux can lead to changes of ocean's salinity and currents (e.g., Schmitz 1996; Murtugudde and Busalacchi, 1998). The region's surface freshwater flux is mainly dominated by the budget of evaporation (E) and precipitation (P). From Fig. 1a, it can be readily seen that the positive E-P attains its maximum at the northern rim of the subtropical gyre (35°N), located slightly northwestward of the area of maximum salinity variability. This displacement demonstrates the potential impact of ocean dynamics on salinity variability. A careful examination of surface wind stress and E-P distributions indicates that a strong northwesterly wind prevails in the E-P maximum region (Fig. 1a). The northwesterly wind drives a positive salinity advection toward the salinity maximum region, thus leading to a southeastward shift of the salinity maximum to the E-P maximum region. In addition, the maximum salinity variability also lies in the regions where the vertical Ekman pumping is predominantly downward (Fig. 1a). The downward Ekman pumping provides a favorable condition for the subduction of high-variability surface waters into the ocean interior.

By transferring the waters from the mixed layer into the ocean interior, subduction is another kinematical and dynamical process coupling the atmosphere and the subsurface ocean. Before proceeding to the calculation of the subduction rate in the northwestern subtropical Pacific, we first examine the winter mixed layer depth

(MLD), which is defined as the depth at which σ_θ increases by 0.125kg.m^{-3} from the surface. As shown in previous studies (Qiu and Huang, 1995; Deser et al., 1996), the winter MLD is generally shallow (~50 m) in the low latitudes and gradually becomes deeper toward the higher latitudes. In the northern subtropical region, near 32°N, the winter MLD reaches up to 150 m from the coast of Japan to ~160°E, lying around the southern edge of the maximum salinity variability. The MLD in the northern subtropical Pacific, as in the other parts of the global ocean, also exhibits a large seasonal variability (figure not shown). After attaining its annual maximum in winter, it begins to decrease rapidly in early spring. The rapid shoaling of MLD allows winter mixed layer waters in the high-variability salinity region to be subducted into the thermocline and be carried to the other regions by the thermocline flows. The annual subduction rate, which is calculated using the MOAA-GPV temperature and salinity data combined with the NCEP wind field, is shown in Fig.1d. It is worth noting that the regions of largest annual subduction rate have been found to roughly coincide with those of the highest salinity variability and deepest MLD (Fig.1b, 1c and 1d). To demonstrate the horizontal transport of the subducted salinity anomalies in the thermocline, we release the passive particles at the base of the mixed layer in February and advect them with the flow field for one year. Figure 1d shows the trajectories of the passive particles in the northwestern subtropical Pacific. The trajectories of these passive particles match well with the contours of the mean Montgomery geostrophic streamfunction on the isopycnals, suggesting that the subducted salinity anomalies in the outcropping regions could be transferred to the western tropical Pacific by a southwestward horizontal flow.

3.2 Propagation pathway

To illustrate where and when the salinity anomalies propagate, an EEOF decomposition is applied to the interannual salinity anomalies on the 24.5-25.2 σ_θ isopycnals with time lags of 1, 3, 5, 7, 9, 11, and 13 months, respectively. The spatial pattern of the first mode (EEOF1) with time lags of 1 month, accounting for ~70.1% of the total variance and explaining a significant part of the salinity variability, is shown in Fig. 2a. To better identify the temporal evolution of the EEOF1, the contour lines of -0.15 PSU with time lags of 1, 3, 5, 7, 9, 11, and 13 months and the corresponding time coefficients are also shown (Fig. 2a and 2b). The first mode captures a low-frequency variability of salinity anomalies in the northwest Pacific, as seen in the time series of the principal component (Fig. 2b). The strongest variance of the first mode is found in the northwestern subtropical region, near 30°N and near 10°N. It should be noted that the salinity anomalies south of 15°N are entirely out of phase with those north of 15°N, displaying a dipolar structure in the northwest Pacific. North of 15°N, a negative anomaly emerges and propagates southwestward from the region south of the Kuroshio Extension toward the western boundary and takes about 13 months to reach the eastern Luzon Strait (see the label number at the contours -0.15 PSU). The southwestward propagation of the signal shows a good correspondence with the PDO index (r=-0.69), which is significantly different from zero at the 95% confidence level (r=-0.596) according to a Student's t test. Compared to the PDO index, the correlation (r=-0.59) between the anomalies and the Nino3.4

index is lower and possibly insignificant during 2003-2012.

The space-time properties associated with the dominant patterns of EEOF1 are similar to those of the regular EOF1 and the lagged correlations in the northwestern subtropical Pacific (Yan et al., 2013), further suggesting that the salinity anomaly, which is related to the PDO, will propagate southwestward to the eastern Luzon Strait. To demonstrate the propagated pathway in more detail, we focus our attention on the latitude-time diagram of salinity anomalies averaged vertically over 24.5-25.2 σ_θ isopycnals along the Montgomery geostrophic streamlines between 28.0 and 29.0 m^2/s^2 (Fig. 2d). The latitude-time diagram of salinity anomalies indicates that the propagated salinity signals exhibit decadal timescale variability and experience two major phase-flipping events in 2005 and 2009. To determine what causes these subsurface salinity changes, we look at the surface salinity anomalies averaged over the subduction region (30°-35°N, 130°-160°E). The two extreme opposing phases of the surface salinity anomalies are found in 2004-2005 and 2009-2010, consistent with the mixed layer salinity variability in the subtropical mode water formation region as shown in Sugimoto et al. (2013). The timing of these peaks nearly coincides with that of the subsurface salinity anomalies, suggesting that the propagation of salinity anomalies along the isopycnals mainly comes from the surface in the outcrop zones.

To see the full cycle of salinity anomalies propagation in the northwestern subtropical Pacific, we plot in Fig. 3 and Fig. 4 the monthly maps of the positive and negative salinity anomalies averaged over 24.5-25.2 σ_θ isopycnals in 2005 and 2009, corresponding to the strongest phase-flipping anomalies as shown in Fig. 2d. A positive salinity anomaly propagates southwestward around the subtropical gyre from Feb 2005 to Jan 2006 (Fig. 3). This anomaly is first detected at 25°-35°N in Feb 2005 (Fig. 3a); it then migrates southwestward approximately along the contours of the Montgomery geostrophic streamfunction and approaches the eastern Luzon Strait at 15°N in Jan 2006 (Fig. 3l). A negative salinity anomaly begins in Feb 2009 (Fig. 4a) and moves along the Montgomery geostrophic streamlines after the positive anomaly. Although propagation of the negative anomalies can be seen farther south of 15°N, the path of this negative anomaly is consistent with that of the positive anomaly (Fig. 4a-4l), demonstrating that the subsurface salinity anomalies in the eastern Luzon Strait are mainly dominated by the surface salinity anomalies in the northwest subtropical outcropping region (30°-35°N, 130°-160°E).

4. Summary and discussion

Using the temperature and salinity datasets provided mainly by the Argo floats, this study provides a detailed description of the subduction and propagation of isopycnal salinity anomalies in the northwest Pacific. By conducting an EEOF analysis and examining two extreme opposing-phase salinity anomalies in 2004-2005 and 2009-2010 along 24.5-25.2 σ_θ isopycnals, we find that salinity anomalies generated in the northwest Pacific subduction region (30°-35°N, 130°-160°E) can propagate to the eastern Luzon Strait via the southwestward subtropical gyre circulations on a time scale of about one year.

The possible connection between the mid-latitudes and the western boundary or the low-latitudes via the subsurface salinity propagation in the North Pacific has been examined in many previous studies (e.g., Ren and Riser, 2010; Sasaki et al., 2010; Li et al., 2012b; Yan et al. 2012; Kolodziejczyk and Gaillard, 2012). Because of the strong along-path dissipation, the salinity anomalies originating in the northeastern subtropical Pacific diffuse quickly as they propagate southwestward and equatorward and nearly vanished before reaching the western boundary (Sasaki et al., 2010; Li et al., 2012b; Kolodziejczyk and Gaillard, 2012). This study shows that salinity anomaly propagation in the northwestern subtropical Pacific is very powerful along its pathway. The anomalies generated in the northwest Pacific outcropping region (30°-35°N, 130°-160°E) are strong and can reach the western boundary. They arrive near the eastern Luzon Strait in about 12 months. This propagation time is faster than the propagation time (about 10 years) observed in the northeast Pacific (Fine et al., 1987; Huang and Liu, 1999; Gu and Philander, 1997; Sasaki et al., 2010) and is consistent with that of subtropical mode water, which is subducted at 30°N and advected southwestward by the Kuroshio Countercurrent to the western boundary (Oka, 2009; Oka and Qiu, 2012; Qiu and Chen, 2013).

Several questions regarding these anomalies remain unanswered. For example, the mechanism of the generation of salinity anomalies in response to the PDO-related atmospheric forcing is not fully resolved. Also, the fate of salinity anomalies upon reaching the eastern Luzon Strait and their downstream impact on the western Pacific warm pool change are still open issues. The western Pacific warm pool, characterized by the warmest seawaters of the global ocean, with sea surface temperatures warmer than 28-29°C, extends from north of 10°N in boreal winter to north of 30°N in boreal summer and is believed to be a key component influencing the number and intensity of tropical cyclones and the onset of El Niño events (e.g., Meinen and McPhaden, 2000; Picaut et al., 2001; Hoerling and Kumar, 2003; Webster et al., 2005; Cravatte et al., 2009). Recent studies have suggested that the warm pool extended both latitudinally and longitudinally during the past decades (Cravatte et al., 2009) and that this extension is not only related to the large-scale air-sea processes but also to the subsurface ocean processes (e.g., Picaut et al. 1996; Qu et al. 2013). Thus, there is some reason to believe that the arrival of the subtropical salinity anomalies into the western boundary may alter the warm pool's thermocline structure and stratification and hence affect its freshwater and heat budget. In the near future, the sustained Argo observations will continue to provide a crucial tool to investigate these issues.

Acknowledgments: This work is partly supported by the National Basic Research Program of China (2013CB430301; 2011CB403504), the Strategic Priority Research Program of the Chinese Academy of Sciences (XDA11010203) and the National Natural Science Foundation of China (41276025).

References

Cravatte, S., T. Delcoix, D. Zhang, M. McPhaden, and J. LeLoup, 2009: Observed freshening and warming of the western Pacific warm pool. Climate Dyn., 33, 565-589.

Deser, C., M. A. Alexander, and M. S. Timlin, 1996: Upper-ocean thermal variations in the North Pacific during 1970-1991. J. Climate, 9, 1840-1855.

Fine, R. A., W. H. Peterson, and H. G. Ostlund, 1987: The penetration of tritium into the tropical Pacific. J. Phys. Oceanogr., 17, 553-564.

Gu, D., and G. S. Philander, 1997: Interdecadal climate fluctuations that depend on exchanges between the tropics and extratropics. Science, 275, 805-807.

Hoerling M, Kumar A, 2003: The perfect ocean for drought. Science 299(5607):691-694.

Hosoda, S., T. Ohira, and T. Nakamura, 2008: A monthly mean dataset of global oceanic temperature and salinity derived from Argo float observations. JAMSTEC Report of Research and Development, 8, 47-59.

Huang, R. X., and B. Qiu, 1998: The structure of the wind-driven circulation in the subtropical South Pacific Ocean. J. Phys. Oceanogr., 28, 1173-1186.

Huang, B., and Z. Liu, 1999: Pacific subtropical-tropical thermocline water exchange in the National Centers for Environmental Prediction ocean model. J. Geophys. Res., 104, 11065-11076.

IOC, SCOR and IAPSO, 2010: The international thermodynamic equation of seawater-2010: Calculation and use of thermodynamic properties. Intergovernmental Oceanographic Commission, Manuals and Guides No. 56, UNESCO (English), 196 pp.

Johnson, G. C., 2006: Generation and initial evolution of a mode water $\theta - S$ anomaly. J. Phys. Oceanogr., 36, 739-751.

Kolodziejczyk, N., and F. Gaillard, 2012: Observation of spiciness interannual variability in the Pacific pycnocline, J. Geophys. Res., 117, C12018, doi: 10.1029/2012JC008365.

Li, Y. L., F. Wang, and F. G. Zhai, 2012a: Interannual variations of subsurface spiciness in the Philippine Sea: Observations and mechanism. J. Phys. Oceanogr., 42, 1022-1038.

Li, Y., F. Wang, and Y. Sun, 2012b: Low-frequency spiciness variations in the tropical Pacific Ocean observed during 2003-2012, Geophys. Res. Lett., 39, L23601, doi: 10.1029/2012GL053971.

Luyten, J., J. Pedlosky, and H. M. Stommel, 1983: The ventilated thermocline. J. Phys. Oceanogr., 13, 292-309.

Meinen C, M. J. McPhaden, 2000: Observations of warm water volume changes in the equatorial Pacific and their relationship to El Niño and La Nina. J Clim., 13: 3551-3559.

Murtugudde, R., and A. J. Busalacchi, 1998: Salinity effects in a tropical ocean model. J. Geophys. Res., 103, 3283-3300.

Montgomery, R. B., 1937: A suggested method for representing gradient flow in isentropic surfaces. Bull. Amer. Meteor. Soc. 18, 210-212.

Oka E., 2009: Seasonal and interannual variation of North Pacific subtropical mode water in 2003-2006. J Oceanogr., 65:151-164.

Oka E., Bo Qiu, 2012: Progress of North Pacific mode water research in the past decade. J Oceanogr., 68: 5-20.

Picaut J, Ioualalen M, Delcroix T, Masia F, Murtugudde R, Vialard J, 2001: The oceanic zone of convergence on the eastern edge of the Pacific warm pool: A synthesis of results and implications for El Niño-Southern Oscillation and biogeochemical phenomena. J. Geophys. Res., 106 (C2): 2363-2386.

Picaut, J., M. Loualalen, C. Menkes, T. Delcroix, and M. J. McPhaden, 1996: Mechanism of the zonal displacement of the Pacific warm pool: Implications for ENSO. Science, 274, 1486-1489.

Qiu, B., and R. X. Huang, 1995: Ventilation of the North Atlantic and North Pacific: Subduction versus obduction. J. Phys. Oceanogr., 25, 2374-2390.

Qiu, B., and S. Chen, 2012: Concurrent decadal mesoscale eddy modulations in the Western North Pacific subtropical Gyre. J. Phys. Oceanogr., 43, 344-358.

Qiu, Bo, Shuiming Chen, 2013: Concurrent Decadal Mesoscale Eddy Modulations in the Western North Pacific Subtropical Gyre. J. Phys. Oceanogr., 43, 344-358.

Qu, Tangdong, Shan Gao, Rana A. Fine, 2013: Subduction of South Pacific Tropical Water and Its Equatorward Pathways as Shown by a Simulated Passive Tracer. J. Phys. Oceanogr., 43, 1551-1565.

Ren, L., and S. C. Riser, 2010: Observations of decadal time scale salinity changes in the subtropical thermocline of the North Pacific Ocean. Deep-Sea Research Part II-Topical Studies in Oceanography, 57, 1161-1170.

Rio, M. H., S. Guinehut, and G. Larnicol, 2011: New CNES-CLS09 global mean dynamic topography computed from the combination of GRACE data, altimetry, and in situ measurements. J. Geophys. Res., 116(C07018), doi: 10.1029/2010JC 006505.

Sasaki, Y. N., N. Schneider, N. Maximenko, and K. Lebedev, 2010: Observational evidence for propagation of decadal spiciness anomalies in the North Pacific. Geophys. Res. Lett., 37, L07708, doi: 07710.01029/02010GL042716.

Schmitz, W. J., 1996: On the World Ocean circulation. Vol. 1: Some global features/North Atlantic circulation. Woods Hole Oceanographic Institute Tech. Rep. WHOI-96-O3, 140 pp.

Sugimoto, S., N. Takahashi, and K. Hanawa, 2013: Marked freshening of North Pacific subtropical mode water in 2009 and 2010: Influence of freshwater supply in the 2008 warm season. Geophys. Res. Lett., 40, 3102-3105, doi:10.1002/grl.50600.

Tomita, H., S. Kako, M. F. Cronin, and M. Kubota, 2010: Preconditioning of the wintertime mixed layer at the Kuroshio Extension Observatory. J. Geophys. Res., 115, C12053, doi: 12010.11029/12010JC006373.

Woods, J. D. 1985: Physics of thermocline ventilation. In Coupled Atmosphere-Ocean Models, ed. by J. C. J. Nihoul, Elsevier.

Webster, P. J, G. J. Holland, J. A. Curry, H. R. Chang, 2005: Changes in tropical cyclone number, duration, and intensity in a warming environment. Science 309(5742):1844-1846.

Yan, Y., D. Xu, Y. Qi, and Z. Gan, 2012: Observations of freshening in the northwest Pacific subtropical Gyre near Luzon Strait. Atmosphere-Ocean, doi: 10.1080/07055900.07052 012.07715078.

Yan, Y., E. P. Chassignet, Y. Qi, and W. K. Dewar, 2013: Freshening of Subsurface Waters in the Northwest Pacific Subtropical Gyre: Observations and Dynamics. J. Phys. Oceanogr., 43: 2733-2750.

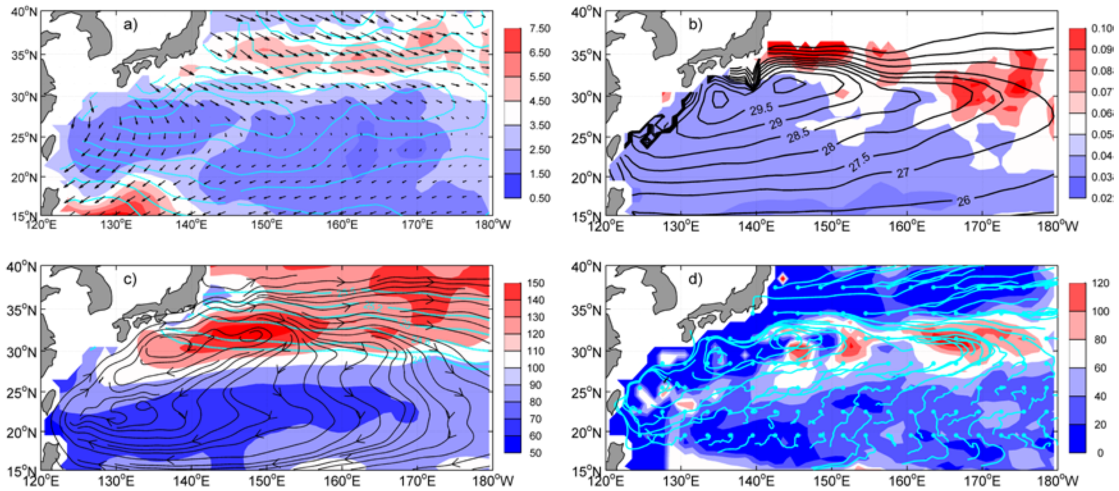

Fig.1: (a) Winter standard deviation (STD) of evaporation minus precipitation (E-P; cm/month) from OAflux and GPCP (shading) with surface wind stress (N.m^2; black arrows) and its curl (N.m^3; cyan contours: solid for positive value, dash for negative value) from CCMP during 2003-2012. (b) Winter STD of salinity anomalies on 24.5-25.2 σ_θ isopycnals (shading) and contours of the mean Montgomery geostrophic streamfunction referred to 2000dbar (m^2/s^2; black contours) on 24.5-25.2 σ_θ isopycnals during 2003-2012. (c) Winter mixed layer depth (m; shading) with 24.5-25.2 σ_θ isopycnal line (cyan contours) and sea surface geostrophic velocity streamlines (black arrows) from AVISO. (d) Annual mean subduction rate (m/year; shading) with Lagrangian trajectories (cyan curves) for a year based on the MOAA GPV data. Here winter months are Dec-Feb.

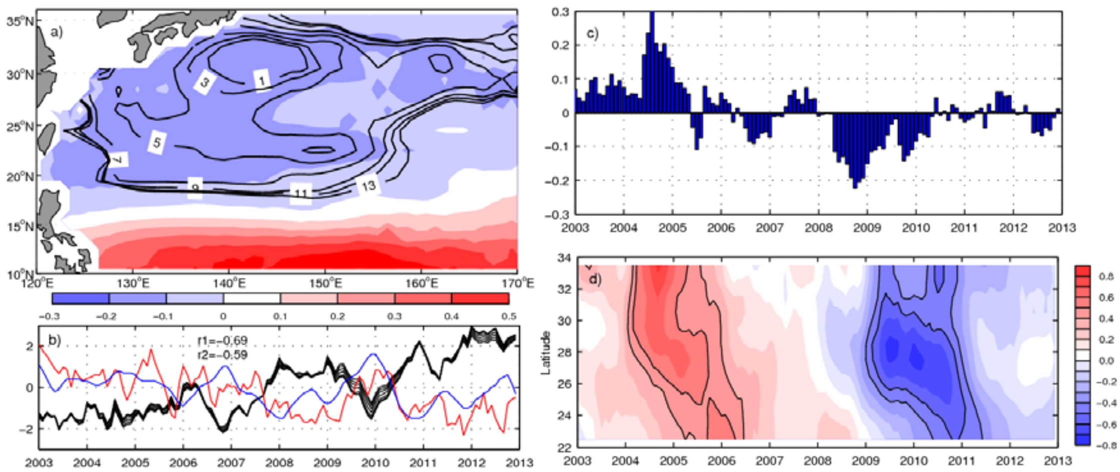

Fig.2: (a) The spatial patterns of the first extended empirical orthogonal function mode (EEOF1) of salinity anomalies (in 10×PSU) averaged over 24.5-25.2 σ_θ isopycnals with time lags 1 months. The contours of -0.15 PSU with time lags 1, 3, 5, 7, 9, 11 and 13 months are highlighted for easy viewing (black curves). (b) The corresponding time coefficients of EEOF1 with time lags 1, 3, 5, 7, 9, 11 and 13 months (black lines), Nino3.4 index (blue line) and PDO index (red line); r1 and r2 is the correlation coefficient between the time coefficients of EEOF1 with time lags 1 month with PDO index and Nino3.4 index, respectively. (c) The surface salinity anomalies averaged over the outcropping region (30°N-35°N, 130°E-160°E). (d) Latitude-time diagram of salinity anomalies (in 10×PSU) averaged vertically over 24.5-25.2 σ_θ isopycnals along the Montgomery geostrophic streamlines between 28.0 and 29.0 m^2/s^2. Contour interval is 0.1PSU, and contours of -0.5, -0.4, 0.4 and 0.5 PSU are marked as black curves.

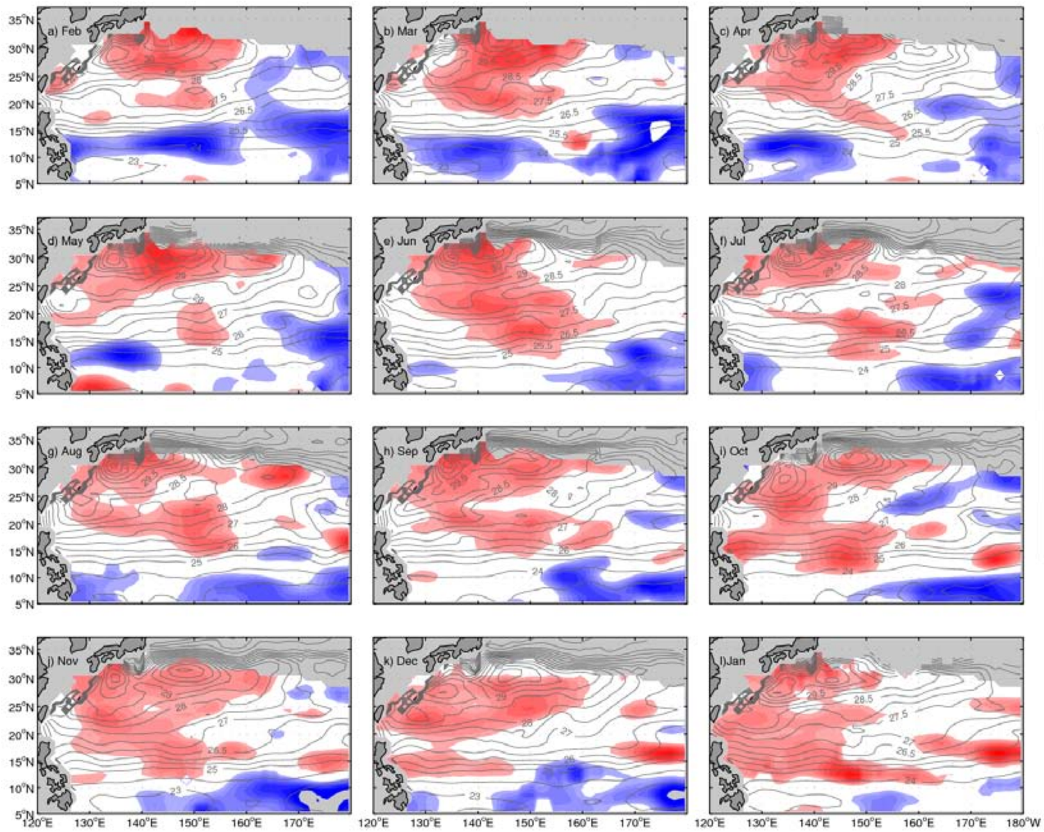

Fig.3: Monthly maps of salinity anomalies averaged over 24.5-25.2 σ_θ isopycnals (shading in 10×PSU) and the corresponding contours of the Montgomery geostrophic

streamfunction referred to 2000dbar for Feb 2005 to Jan 2006 (gray contours) based on the MOAA GPV data.

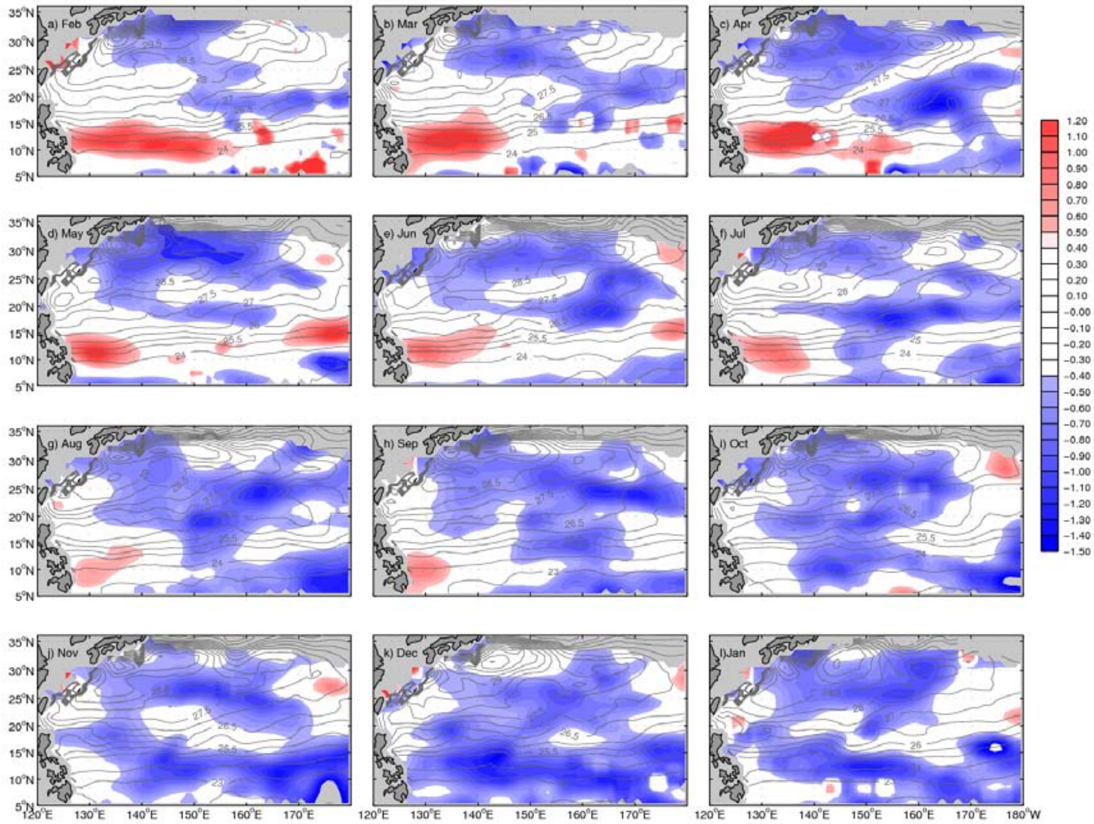

Fig.4: Same as Fig.3 bur for Feb 2009 to Jan 2010.